COMBINED MICROFLUIDIC SINGLE-CELL ELECTROPORATION AND IMPEDANCE SPECTROSCOPY ANALYSIS

Sebastian C. Bürgel[1], Carlos Escobedo[1], Simon Kemmerling[2], Nora Sauter[2], Niels Haandbæk[1], Olivier Frey[1] and Andreas Hierlemann[1]

[1]ETH Zürich, Department of Biosystems Science and Engineering, Basle, Switzerland
[2]Universität Basel, Center for Cellular Imaging and Nano Analytics, Basle, Switzerland

ABSTRACT

Most current systems for cell-electroporation are based on bulk-processing of large quantities of cells. Typically, fluorescent labels are required to assess the performance of these systems. We aim at designing a system for controlled single-cell electroporation and label-free assessment of the process through impedance spectroscopy.

Here we investigated a microsystem that utilizes electrical impedance spectroscopy (EIS) to analyze on-chip electroporation. The performance of this system was evaluated by using the mammalian cell line BHK-21. The electroporation process of the cells was observed by fluorescent microscopy and simultaneously through EIS at high temporal resolution. EIS measurements revealed significant differences in the signals of a cell before and after irreversible poration. Additionally, EIS allowed for insights into the re-sealing dynamics of reversible electroporation of single cells.

KEYWORDS

electroporation, impedance spectroscopy, microfluidics, single cell analysis

INTRODUCTION

The porating effect of high electric fields on the cell membrane has been known for a long time. It was first used to kill cells [1] and later to introduce foreign DNA fragments into cells for transfection [2]. Weaker electric fields can be used in EIS, which is a label-free method to measure the electrical properties of micro-particles and cells in a solution [3].

Here, we present an integrated microsystem for both, EIS and electroporation of single cells. Our approach towards the development of a single-cell total analysis platform, depicted in Figure 1, includes EIS analysis and bidirectional flow-control via a syringe pump. The system enables label-free analysis of free-flowing single cells over extended time by shuttling them back and forth through a region equipped with microelectrodes. This scheme offers important advantages over established techniques: (1) no need to trap cells, (2) time-resolved measurements of single-cell properties and (3) simplicity of device design, fabrication, and operation.

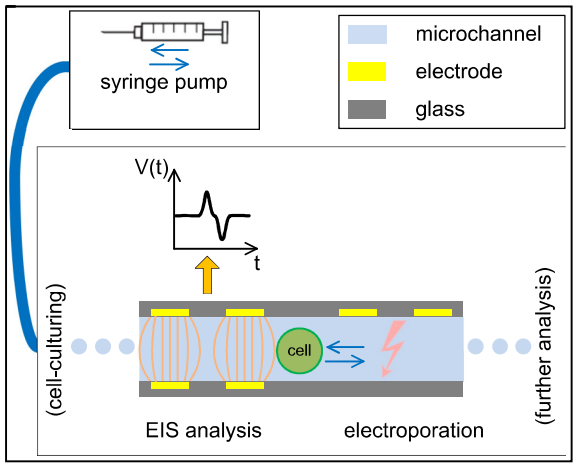

Figure 1: Schematic side view of the presented microsystem. A syringe pump is used for shuttling a cell back and forth through the EIS analysis region. When switching on the electrodes, the cell gets electroporated while the EIS signal is continuously recorded. Possible integration of cell-culturing and hand-over to perform further analysis steps are indicated.

EXPERIMENTAL

Figure 2 shows a schematic of the experimental setup. EIS measurements and electroporation were achieved by separate sets of opposing and coplanar microelectrodes. We used baby hamster kidney cells (BHK-21), suspended in medium containing fluorescein diacetate (FDA) and propidium iodide (PI) dyes to assess cell viability and electroporation efficiency. Individual cells were shuttled back and forth through the measurement and electroporation region using a syringe pump. Each time a cell passed the measurement electrodes, the impedance spike of the cell was recorded using a HF2IS impedance spectroscope (Zurich Instruments AG, Switzerland), which was also used to generate a field strong enough to electroporate the cell.

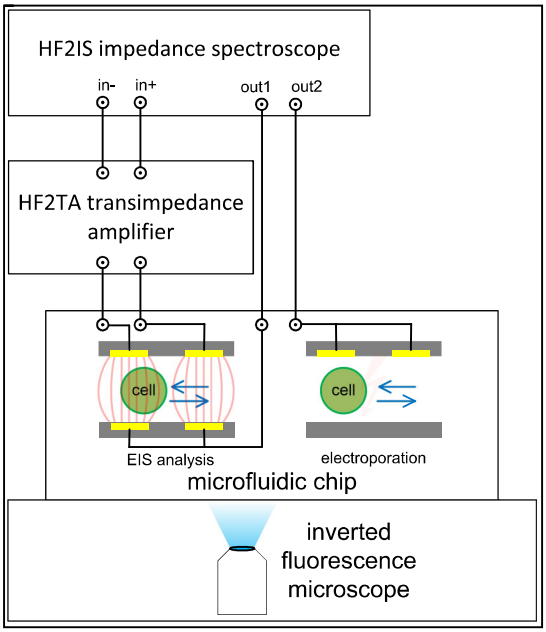

Figure 2: A microfluidic chip is placed on top of an inverted fluorescence microscope. Electric signals from a HF2IS impedance spectroscope are used inside the chip for electroporation (right) and EIS measurements (left). The signal of a cell passing between electrodes (field lines sketched in red) is processed in the HF2IS impedance spectroscope behind a HF2TA transimpedance amplifier.

RESULTS

Figure 3 (top) shows phase contrast images of a BHK-21 cell before and after exposure to a poration field of 5.5 kV/cm at 1 kHz. The cell shows a dramatic morphological change, with ~ 300% increase in volume. To confirm cell electroporation, fluorescence analysis was performed. Figure 3 (center) shows decreasing fluorescence intensity during 0.5 s for a cell stained with the cell viability dye FDA, demonstrating that the cell is no more alive. Figure 3 (bottom) shows a fluorescence intensity increase for PI staining of a viable cell during 20 s, which confirms successful electroporation and cell death.

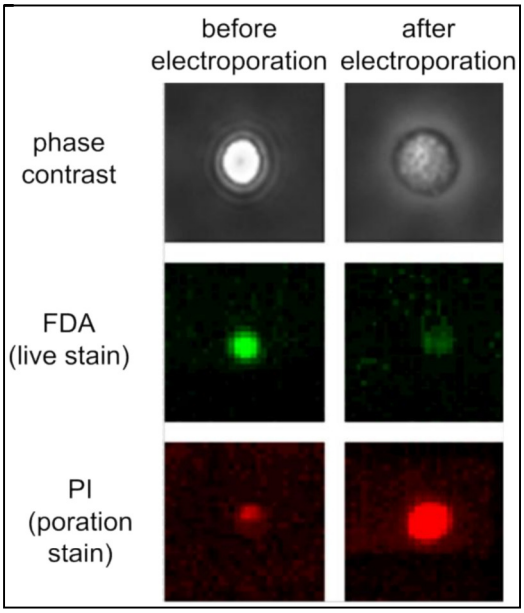

Figure 3. Images of cells before (left) and after (right) irreversible electroporation. Top: Phase contrast image, center: FDA staining of living cells, bottom: PI staining of dead cells with broken membrane. Imaging parameters were the same before and after electroporation.

Figure 4 shows 3.8 MHz impedance signals, recorded for additional, label-free electroporation assessment. The impedance signal of Figure 4 (top) corresponds to irreversible electroporation of a viable cell. The cell was shuttled four times through the measurement region prior to electrical treatment. Clear spikes are observed in the real component of the complex impedance (15µV), when a cell passes the inter-electrode region, but just very small spike amplitudes are seen in the imaginary component (2µV). After applying the fatal electroporation field, the

signals are opposite: The amplitudes of the imaginary part increase 4-fold, and there is no detectable signal in the real part of the signal. This observation can be explained by drastic changes in the membrane potential and cytosol conductivity of the cell caused by the poration opening the cell membrane. The effects in the impedance signal for reversible electroporation at 4.4 kV/cm and 5 kHz are shown in Figure 4 (bottom). A cell is measured five times and then electroporated, at which point a reduced spike amplitude can be detected; the spike amplitude, however, completely recovers within a few seconds. This is in agreement with the re-sealing dynamics observed in other mammalian cells after electroporation [4].

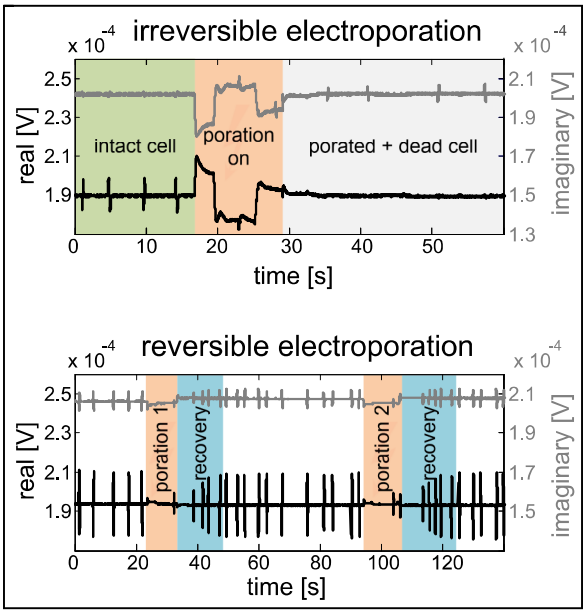

Figure 4. Top: Multiple impedance measurements of the same cell, shuttled back and forth before (spikes in real part) and after irreversible electroporation (spikes in imaginary part). Bottom: Two mild electroporation treatments of one cell with recovery (amplitude of spikes recovers) within several seconds. The reversibly electroporated cell is bigger than the irreversibly electroporated one, therefore both the real and the imaginary spike amplitudes are bigger for the reversibly electroporated cell.

CONCLUSION

We report on a microsystem featuring electroporation and impedance-based analysis units for single free-flowing cells. Successful electroporation was analyzed by EIS, the results of which were in agreement with fluorescence analysis. Repeated measurements enabled by bidirectional flow (back-and-forth) of the same cell revealed reproducible cellular recovery within a few seconds.

ACKNOWLEDGEMENTS

The authors acknowledge financial support through the Swiss Systems Biology Program “SystesmsX.ch” within the RTD Cellular Imaging and NanoAnalytics (CINA).

REFERENCES

[1] A. Sale and W. Hamilton, *Effects of high electric fields on microorganisms I. Killing of bacteria and yeasts*, Biochimica et Biophysica Acta - General Subjects, 148(3), pp. 781-788, (1967).

[2] E. Neumann, M. Schaefer-Ridder, Y. Wang, P. H. Hofschneider. Gene transfer into mouse lyoma cells by electroporation in high electric fields, The EMBO journal, 1(7), pp. 841-845, (1982).

[3] S. Gawad, K. Cheung, U. Seger, A. Bertsch and P. Renaud, *Dielectric spectroscopy in a micromachined flow cytometer: theoretical and practical considerations*, Lab on a chip, 4(3), pp. 241-251, (2004).

[4] K. Kinosita, T. Y. Tsong, *Formation and resealing of pores of controlled sizes in human erythrocyte membrane,* Nature, 268(5619), pp. 438-441, (1977).

CONTACT

Sebastian Bürgel: +41 61 387 3298 or sebastian.buergel@bsse.ethz.ch